EasyChair Preprint

№ 4259

Multi-Target Tracking and Detection, fusing RADAR and AIS Signals using Poisson Multi-Bernoulli Mixture Tracking, in support of Autonomous Sailing

Tianlei Miao, Ehab El Amam, Peter Slaets and Davy Pissoort

September 25, 2020

Multi-Target Tracking and Detection, fusing RADAR and AIS Signals using Poisson Multi-Bernoulli Mixture Tracking, in support of Autonomous Sailing

Tianlei Miao[ab*], Ehab El Amam[b], Peter Slaets[a], Davy Pissoort[a]

[a]*KU Leuven, Belgium;* [b]*RH Marine Netherlands B.V., the Netherlands*

[*]Corresponding author. Email: tianlei.miao@rhmarine.com

Synopsis

To sail safely, an autonomous vessel should be able to keep track of the position and motion of other vessels and obstacles, which refers to the multi-target tracking problem. Furthermore, RADAR and automatic identification system (AIS) are two sensors commonly used onboard for tracking maritime targets. The fusion of these two sensors, utilizing complementary information and handling the conflicting data, gets increasingly important during autonomous sailing. However, due to the immaturity of multi-target tracking methods, the fusion was hardly systematically discussed, when there are missed detections from certain single sensors and conflicts between two sensors. As the new multi-target tracking methods have been proposed, this paper first presents a sequential measurement-level fusion approach of RADAR and AIS based on the newest random finite set (RFS)-based filter — Poisson multi-Bernoulli mixture (PMBM) filter. The comparison of the performance both using sequential fusion and using the sensor information individually is presented in this article. Then the proposed sequential fusion of RADAR and AIS based on PMBM filter was applied to a real maritime case. The tracking results are given and the performance is analyzed.

Keywords: RADAR and AIS fusion; sensor fusion; multi-target tracking; PMBM tracker; data association

1 Introduction

To ensure safe autonomous sailing, an autonomous vessel should be able to keep track of the position and motion of other vessels and obstacles. With such objective, multi-target tracking (MTT) has become a key aspect of autonomous sailing, as it allows to cope with the real dynamic environment with multiple targets around the own vessel. Besides, fusing the multiple sensors on board gives a possibility to improve the robustness and reliability of the MTT problem, as opposed to using single sensors. Thus, in this paper, a sensor fusion approach within the multi-target tracking problem is presented. Moreover, this approach has been applied to measured RADAR / AIS data from a real case. The output of the multi-target tracking will be used as input to a collision avoidance algorithm (The collision avoidance algorithm is beyond the scope of this paper).

Multi-target tracking (MTT) involves jointly estimating both the number and states of the targets from possibly noisy sensor measurements. The main ongoing challenge is data association, which aims to associate measured data with certain target. These targets can be known targets (previously detected), new targets (not previously detected) or non-existing targets (clutter) upon the arrival of new sensor data. Apart from that, sometimes sensors may not capture any measurements from existing targets. Thus, data association has been playing a highly important role within the multi-target tracking problem. However, data association can be computationally expensive when dealing with multiple targets and is further complicated by uncertainty in measurement origin and target position.

Through the years, several approaches have been proposed to handle the data association problem in MTT. The two traditional major approaches are joint probabilistic data association (JPDA)[1] and multiple hypothesis tracking (MHT)[2]. JPDA marginalizes over the random variables representing the association in order to calculate the marginal distribution of each track. MHT seeks to find the maximum a posteriori (MAP) correspondence over a recent history of the association to calculate the most likely hypothesis.

In recent years, a new statistical framework called random finite set(RFS) or finite set statistics (FISST) is widely used to model the MTT problem in a Bayesian way[3]. Here, the usual setup is to consider the state of the system as a set of targets. It has shown to be a good systematic framework for MTT, giving a top-down formulation for solving the MTT problem[4]. Various RFS-based filters have been proposed and extended during

Authors' Biographies

Tianlei Miao currently is a Ph.D. researcher at the Catholic University of Leuven and RH Marine on ensuring autonomous sailing from A to B. His research interests include data fusion, multi-target tracking, and collision avoidance in autonomous sailing. He has previously received a joint master degree in Maritime Engineering at both Norwegian University of Science and Technology and Royal Institute of Technology.

Ehab El Amam is an engineering consultant at RH Marine Netherlands B.V., the Netherlands. His expertise includes dynamic position system, autopilot system, and energy management system.

Peter Slaets is an associate professor in Robotics, Automation, and Mechatronics(RAM) at the Faculty of Engineering Technology, Catholic University of Leuven. His research interests include autonomous localization, navigation, embedded hardware, and sensor fusion.

Davy Pissoort is an associate professor in Telecommunications and Microwaves at Faulty of Engineering Technology, Catholic University of Leuven. His research interests include autonomous systems, system safety, electromagnetic compatibility, and electromagnetic interference.

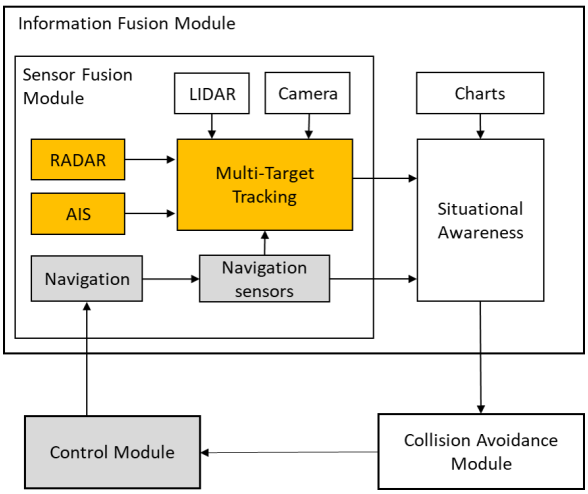

Figure 1: Block diagram of the system architecture for the autonomous sailing research. Orange blocks are focused upon this paper. Gray blocks are out of the scope of this research.

the last decade, including probability hypothesis density (PHD)[5], cardinalized PHD (CPHD) filters for standard models[6], multi-target multi-Bernoulli (MeMBer) filter[7] and labelled RFS filters[8].

Different from the (C)PHD and MeMBer filters, the Poisson multi-Bernoulli mixture (PMBM) filter[9] has a closed-form filtering recursion based on standard state-space models with Poisson target birth and has shown a better performance than other RFS-based filters[10, 11]. It separates the set of objects into two disjoint subsets: objects that have been detected modelled by multi-Bernoulli mixture (MBM), and objects that have not yet been detected, modelled by Poisson Point Process (PPP). PPP enables the filter more sensitive to target birth than the Bernoulli birth while the MBM considers different track-measurement-association hypotheses gaining a higher accuracy than a single multi-Bernoulli[11]. In this way, the PMBM is able to give a model rather close to the real case with respect to changing and time-varying number of targets.

The utilization of multiple sensors is another key aspect to improve the robustness and reliability of MTT for autonomous sailing. Fundamentally, there are several sensors that can provide information to autonomous vessels for the MTT problem. One is the automatic identification system (AIS), through which ships can broadcast static information (e.g. MMSI number, IMO number, ship name), dynamic information (e.g. position, speed), and other relevant information to each other. The vessels can also perceive their environment including other ships by means of exteroceptive sensors such as RADAR, lidar, and camera. In this paper, AIS and RADAR are used as two sources in the specific MTT scenarios. The dynamic information from AIS has relatively high data accuracy since it uses the global position system (GPS) on the corresponding target vessel. However, only vessels over a certain size are obliged to have AIS, and AIS can be turned off due to various reasons and sometimes spoofed. Compared with AIS, RADAR works on a simple principle: detection based on the returned RADAR echos. Using RADAR, the vessel can not only detect other vessels but also other objects, like buoys. But sometimes there is too much clutter using a RADAR, due to unwanted echoes bouncing off the target, and a RADAR antenna may not detect occluded objects. Therefore, relying on a single sensor is not sufficient in terms of reliability and safety due to each sensor's inherent drawbacks and limitations. How to make full use of complementary sensor data and resolve possible conflicts becomes a key aspect of sensor fusion.

There have been quite some achievements concerning sensor fusion in the field of maritime multi-target tracking in recent years. Hermann et al.[12] fused RADAR target data and camera data using global nearest neighbour (GNN) to perform obstacle detection and tracking for unmanned surface vehicles. They found that sensor fusion significantly increased obstacle tracking performance. A measurement level sensor fusion system using LIDAR, RADAR, electro-optical and infrared cameras with joint integrated probabilistic data association (JIPDA) for maritime MTT was demonstrated in [13]. In [14], a method was proposed for online tracking multiple targets with multiple Doppler RADARs using generalized labeled multi-Bernoulli (GLMB) filter. Outside the maritime domain, several papers have addressed heterogeneous sensor fusion for cars[15] and medical robots[16]. As PMBM filter was proposed and proven to have a better performance than other RFS-based filters for MTT problem[10], applying sensor fusion with the PMBM filter is certainly promising.

The remainder of this article is organized as follows. Section 2 presents the background of the RFS framework. In Section 3, we review the single sensor PMBM filter and present a multi-sensor extension of the PMBM filter. Simulations and a real-case application using a multi-sensor PMBM filter and their results are presented in Section 4, followed by concluding remarks and future work in Section 5.

2 Background

This section summarizes the multi-object state space models and Bayesian filtering recursion within the RFS framework. A RFS of the multitarget states is denoted by a set $X = \{x^1, x^2, \cdots, x^i, \cdots, x^n\}$, where $n = |X|$ is the cardinality, and $x^i \in \mathbb{R}$ is the state vector of the i-th target. Both the distribution over cardinality and the distribution over the elements of the multitarget set X are captured by its probability density function (pdf), denoted by $f(X)$. For any realization $X = \{x^1, x^2, \cdots, x^i, \cdots, x^n\}$ with a given cardinality $|X| = n$, its pdf[4, p. 84] is

$$f(X) = n!\rho(n) f_n(x^1, ..., x^n) \tag{1}$$

where the cardinality distribution is $\rho(n) \triangleq Pr\{|X| = n\}$ and $f_n(x^1, ..., x^n)$ is an ordered multi-target pdf with non-set states input.

Within the RFS framework, a birth model of new targets can be built to describe the possibility of new targets appearing at each time point by using the Poisson Point Process (PPP). That is, at time k, a possibly empty set of new-born targets X_k^B appears, distributed as a PPP with intensity $\lambda_k^B(x_k)$. The birth cardinality then is denoted by a Poisson probability mass function(pmf)[9], with the rate $\bar{\lambda}_k^B$,

$$\rho^B(n) = e^{-\bar{\lambda}_k^B} \frac{(\bar{\lambda}_k^B)^n}{n!} \tag{2}$$

where $\bar{\lambda}_k^B = \int \lambda_k^B(x_k) dx_k$ and $\mathbb{E}[|X|] = \bar{\lambda}_k^B$. The pdf of new-born targets RFS yields a multi-dimensional Poisson distribution[17],

$$f(X^B) = e^{-\bar{\lambda}_k^B} \prod_{i=1}^{n} \lambda^B(x_i) \tag{3}$$

Where $\lambda^B(x)$ is the pdf of a single target. Considering that the birth of each new target is assumed independent of each other, a product of single target pdfs is used as multi-target pdf. Moreover, a fixed label set $L = \{l^1, ...l^n\}$ can be introduced[4, p. 446] when every new target is born, which helps to distinguish individual targets in a multi-target state[17]. The label l^i for i-th target is unique. Then the combined state set of labeled targets has the form

$$\mathring{X} = \{\mathring{x}^1, ..., \mathring{x}^n\} = \{(x^1, l^1), ..., (x^n, l^n)\} \tag{4}$$

Correspondingly, the object death, i.e., when the object leaves the surveillance area or disappears, is described by modeling object survival, which is independent of target birth. The object survival rate, or namely the probability that an object with state x_{k-1} survives to the next time step k, is $P^S(x_{k-1})$. In contrast, the death rate is $1 - P^S(x_{k-1})$. Thus, the surviving process of each target is a Bernoulli process, independent of the other targets. Each survival target attains a new state x_k according to a Markov jump pdf $f_{k|k(x_k|x_{k-1})}$ [18].

It is possible that a target is not detected by a certain sensor or detector at some moment so that the process of detection can be also modeled as a Bernoulli process. Given a target with sate x_k, one sensor can either detect it with probability $P_k^D(x_k)$ and generates a measurement $z_k \in Z_k$ with likelihood $l_k(Z_k|x_k)$ or fail to detect it with probability $1 - P_k^D(x_k)$, where Z_k denotes the set of measurements received at time k.

2.1 Standard Motion Model

The motion model works for the prediction of the surviving targets and new-born targets. Given the RFS of target states from last time step X_{k-1}, the RFS of current time step k is

$$X_k = X_k^S \uplus X_k^B \tag{5}$$

where X_k^S is the surviving targets RFS from the last time step, X_k^B is the new-born targets RFS at time k. The symbol $\uplus$ means two sets are mutually disjoint. The complete motion model is

$$f(X_k|X_{k-1}) = \sum_{X_k^B \uplus X_k^S = X_k} f_k(X_k^B) \boldsymbol{\pi}_k(X_k^S|X_{k-1}) = \sum_{X_k^B \uplus X_k^S = X_k} f_k(X_k^B) \prod_{i=1}^{n_{k-1}} \boldsymbol{\pi}_k(X^{S,i}|\{x_{k-1}^i\}) \tag{6}$$

where the birth model is a Poisson RFS given as (3) and the surviving target model is a product of a single target motion model due to the independence of the motion model of all targets. The single motion model is also a Bernoulli

$$\boldsymbol{\pi}_k(X^S|\{x\}) = \begin{cases} P^S(x)\pi_k(x^s|x) & \text{if } X^S = \{x^s\} \\ 1 - P^S(x) & \text{if } X^S = \emptyset \\ 0 & otherwise \end{cases} \tag{7}$$

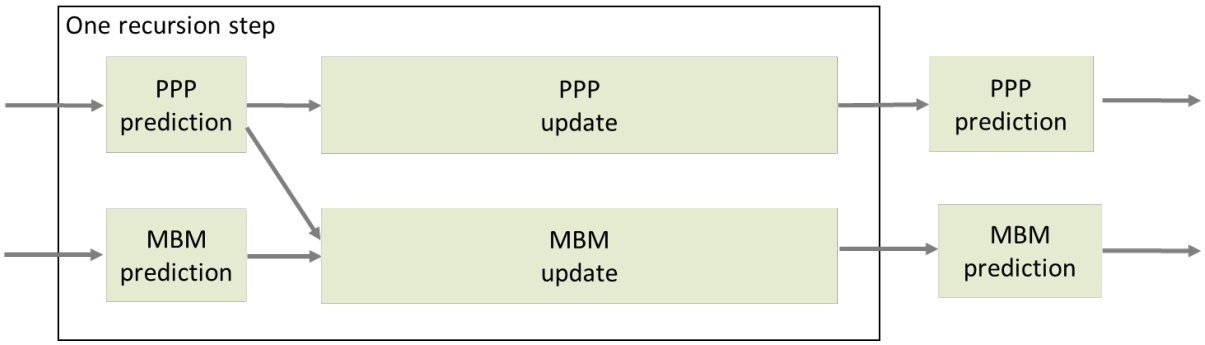

Figure 2: Single-sensor PMBM filter prediction and update flow chart

2.2 Standard Point Target Measurement Model

Point target assumption is used in this paper which means that each target can at most generate one measurement for each sensor at each moment. The measurements can either originate from clutter or targets. Given the set $X = \{x^1, x^2, ..., x^n\}$ of targets, the set Z of measurements is $Z^c \uplus Z^1 \uplus Z^2 \uplus ... \uplus Z^n$, where Z^c, Z^1,...Z^n are independent sets. Z^c is the set of clutter measurements, modelled as a Poisson Point Process with indensity $\lambda^c(Z^c)$, similar to the birth model3. Z^i is a (possible empty) set of measurements produced by target i [4]. The complete measurement model is expressed as

$$f(Z_k|X_k) = \sum_{Z^c \uplus Z^1 \uplus Z^2 \uplus ... \uplus Z^n} f_{Z^c}(Z^c) \prod_{i=1}^{n^k} \boldsymbol{g}_k(Z^i|x_k^i) \tag{8}$$

where $f_{Z^c}(Z^C)$ is the pdf of as a PPP, similar as [3] and $\boldsymbol{g}_k$ is the single measurement model

$$\boldsymbol{g}_k(Z|\{x\}) = \begin{cases} P^D(x) g_k(z|x) & \text{if } Z = \{z\} \\ 1 - P^D(x) & \text{if } Z = \emptyset \\ 0 & otherwise \end{cases} \tag{9}$$

2.3 Bayesian Filtering with RFS

Bayesian filtering recursion with RFS consists of the usual prediction and update steps. Prediction and update are given according to the Chapman-Kolmogoroc equation[18] and Bayes' rule, respectively,

$$\begin{aligned} prediction \quad & f(X_k|Z_{1:k-1}) = \int f(X_k|X_k - 1) f(X_k - 1|Z_{1:k-1}) \delta X_{k-1} \\ update \quad & f(X_k|Z_{1:k}) = \frac{f(Z_k|X_k) f(X_k|Z_{1:k-1})}{\int f(Z_k|X_k') f(X_k'|Z_{1:k-1}) \delta X_k'} \end{aligned} \tag{10}$$

where $f(X_k|Z_{1:k-1})$ and $f(Z_k|X_k)$ are the motion model and measurement model mentioned before.

3 Sensor fusion within PMBM filter

In this section, we review the single-sensor PMBM filter and extend it to the multi-sensor case with a sequential fusion approach.

3.1 Poisson Multi-Bernoulli Mixture filter

Poisson multi-Bernoulli mixture (PMBM) divides the targets into two groups: undetected targets (hypothesized to exist but not previously detected) and detected targets, and use Poisson Point Process and Multi-Bernoulli Mixture model to describe the two parts, respectively. A notion of potential targets (PTs) is introduced to denote the union of these two groups. Based on the standard state-space model assumptions, PMBM conjugacy prior is given by [9],

$$f^{PMBM}(X) = \sum_{X^U \uplus X^D = X} f^P(X^U) f^{MBM}(X^D) \tag{11}$$

where superscripts U and D represent the undetected targets group and detected targets group, respectively. Function $f^p(\cdot)$ is the PPP component expressed as

$$f^P(X^U) = e^{\bar{\lambda}^U} \prod_i^{n_k} [\lambda^U(x_k^i)] \tag{12}$$

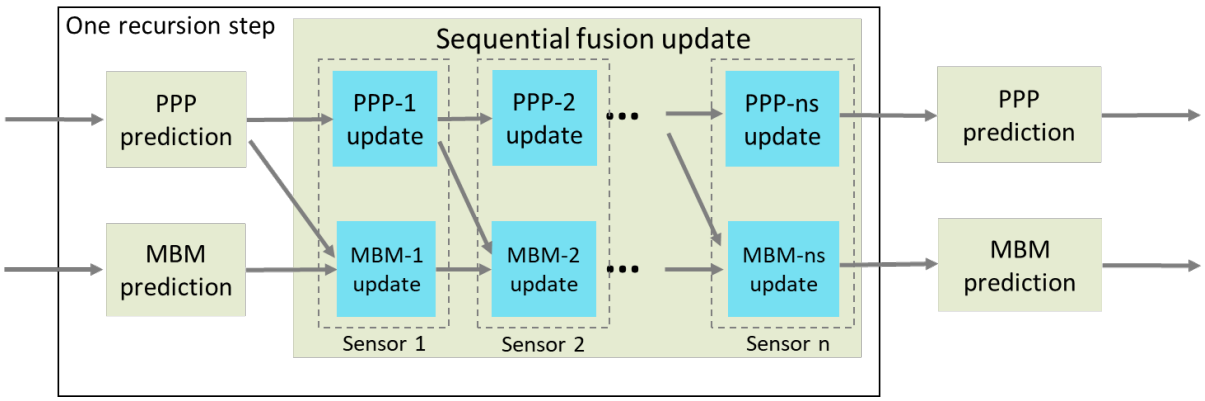

Figure 3: Sequential fusion pattern of multi sensors using PMBM filter

where λ^U denotes the intensity of PPP component for undetected targets. The MBM component, $f^{MBM}(\cdot)$, is expressed as

$$f^{MBM}(X^D) \propto \sum_j \sum_{X_1^D \uplus X_2^D \uplus \ldots \uplus X_n^D = X^D} \prod_{i=1}^{n} w_{j,i} f_{j,i}(X_i^D) \tag{13}$$

where $\propto$ stands for proportionality, j is an index over all global hypotheses (components of the mixtures)[9], n is the number of potentially detected targets, and $w_{j,i}$ and $f_{j,i}(\cdot)$ are the weight and the Bernoully density of detected target i under the j-th global hyopothesis. Details for predicting and updating both PPP and MBM are provided in [9] and [19], which is omited here.

With the assumption of independence of the undetected group and the detected group, the PPP component and MBM component can be separately calculated. Despite this, PMBM follows the same rule as Bayesian filtering recursion using prediction and update steps to calculate the pdf of multi-targets at the current moment. Regarding the update step, it is possible that a previously undetected target is first-time detected which involves the move from undetected group to the detected group. As such, the PPP prediction results are passed to the MBM update. Figure 2 gives the flow chart of one recursion step of PMBM.

3.2 Sensor Fusion with PMBM Filter

Considering a general multi-sensor tracking system composed of sensors s = 1,2,...,n_s with identical fields of view, it is quite natural that we continue to use the existing result of single-sensor PMBM filter for the multi-sensors case. However, the manner that directly applies one PMBM filter for each sensor brings extra computation complexity since one more dimension of association is introduced when we try to fuse the results of different PMBM filters. Although a distributed fusion system with multiple calculation units can accelerate the computational time, sequential fusion is a potential way to realize the fusion with regard to a centralized system[20].

Using the sequential fusion of multiple-sensor PMBM ($n_s \geq 2$), the prediction step in Bayesian filtering recursion (10) is unchanged as it does not involve any measurements. Only the motion model and the posterior from the last step are involved. Regarding the update step, using (10), for simplicity, the denominator can be removed since it is constant. The equal sign is replaced by the proportional sign as written in the first line in 14. With the assumption that measurement models of different sensors are conditionally independent of each other when given the multi-target state RFS, one obtains

$$\begin{aligned} f(X_k|Z_{1:k}) &\propto f(Z_k|X_k) f(X_k|Z_{1:k-1}) \\ &= (\prod_{s=1}^{n_s} f(Z_{k,s}|X_k)) f(X_k|Z_{1:k-1}) \end{aligned} \tag{14}$$

Based on this expression, the update step can be performed sensor-sequentially within an iterated-update method. Iterated marginal posterior pdfs $f(X_k|Z_{1:k}^s)$ are calculated for each sensor $s = 1, \cdots, n_s$, where $f(X_k|Z_{1:k}^s)$ denotes the pdf of X_k conditioned on $Z_{1:k-1}$ and $Z_{k,s'}$ for $s' = 1, \ldots, s$. Through the s-th update step, $f(X_k|Z_{1:k}^{s-1})$ is converted into $f(X_k|Z_{1:k-1})$, thereby incorporating the measurement $Z_{k,s}$ of sensor s. The initial step of this recursion is $f(X_k|Z_{1:k}^0) = f(X_k|Z_{1:k-1})$, which starts with the posterior from the last time step. The s-th update step is basically equal to the single-sensor update step discussed in Section 2. The only differences are that the input $f(X_k|Z_{1:k-1})$ of the single-sensor update steps is replaced by $f(X_k|Z_{1:k}^{s-1}|)$, and the measurements Z_k^m, $m \in \{1, \ldots, M_k\}$ are replaced by $Z_{k,s}^m$, $m \in \{1, \ldots, M_{k,s}\}$. The flow chart of this sequential fusion is shown in Figure 3.

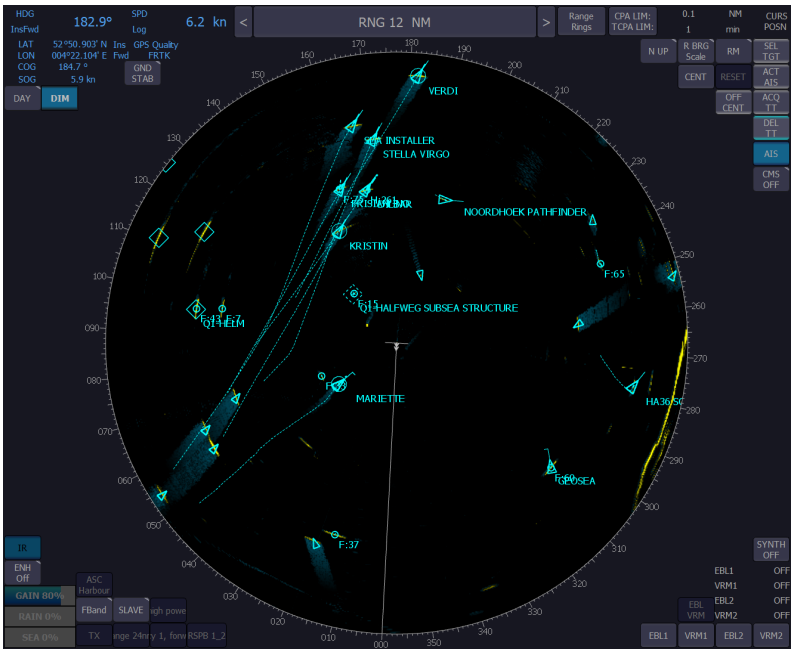

Figure 4: One scenario extrated from the record of a sea trial displaying by a RADAR system

Due to the performed approximation, a sensor-sequential update can lead to a poorer performance than using a single sensor with certain set-type filters, such as the PHD, CPHD, and MeMber filters[20]. But, using PMBM, this problem is supposed to be avoided since PMBM can give a closed-form solution without any extra approximations. Meanwhile, theoretically, the updating order of different sensors should not be a problem with a PMBM filter regardless of the post-processing. In Section 4, we verify the influence of the sensor order using PMBM. Although the computational load is increasing compared to the single-sensor case due to the iterations of updates for multiple sensors, no extra increased loads are involved in the prediction step.

4 Simulation and Application

In this section, we first implement RADAR and AIS sequential fusion based on a PMBM filter for a simulation scenario and then evaluate the performance by the mean generalized optimal subpattern assignment (GOSPA). After that, we apply this fusion approach to a real maritime case, which is part of the recording of a real sea trial.

4.1 Problem formulation

The problem is based on the scenario given in Figure 4 during a real sea trial: the own ship (in the center) was sailing near a sea lane, where several target ships were sailing. Besides, there were other ships sailing in the proximity with various directions and there were some static maritime platforms. The motion of most targets was nearly constant in this scenario. During the 30-minute monitoring period, crossing between target vessels, close sailing, and separating happened. A 3-band RADAR (F-band, I-band, and F-Heli) and an AIS were used during the trial with the assumed same field of view(FOV). The pre-processed RADAR data containing the dynamic state based on the point-target assumption of potential targets is used (shown as a small circle). The data from 3 different bands can be obtained separately so that we consider it as 3 different data sources during the fusion. AIS as a sensor can detect the same-type dynamic state of most target ships (shown as an oriented triangle). But some target ships are not equipped with an AIS. So in that case those targets are not possible to be detected by AIS at all. The detection of RADAR with 3 bands can be missed at some sample time due to certain factors such as occlusion. Both RADAR and AIS might detect clutters due to certain reasons.

4.2 Simulation

In order to evaluate the performance of the multi-sensor PMBM filter, a simulation scenario similar to the real scenario was considered first, monitored by a fixed sensor network consisting of 3 RADARs and an AIS. All 3 RADARs and AIS have the same FOV which is a circle with a radius of 10 nautical miles (1 nm = 1852 m). In the simulation scenario, the center of the FOV is fixed at $[0,0]$ in order to exclude the influence of uncertainty from the own ship position. In total, 10 targets are generated with various states, trajectories, birth time step, and death time step, as shown in Figure 5. Among them, target 8 is static, simulated as an offshore platform; target

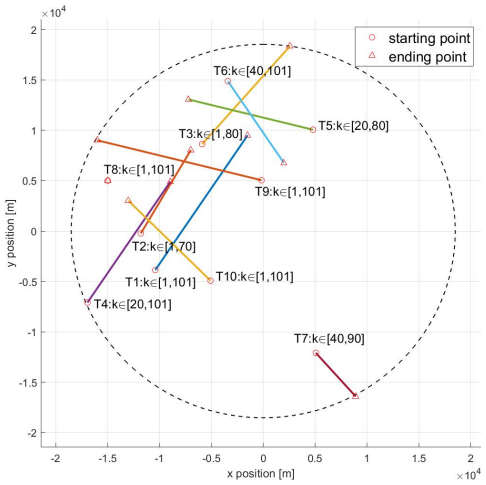

Figure 5: Simulation scenario consists of 10 tartgets

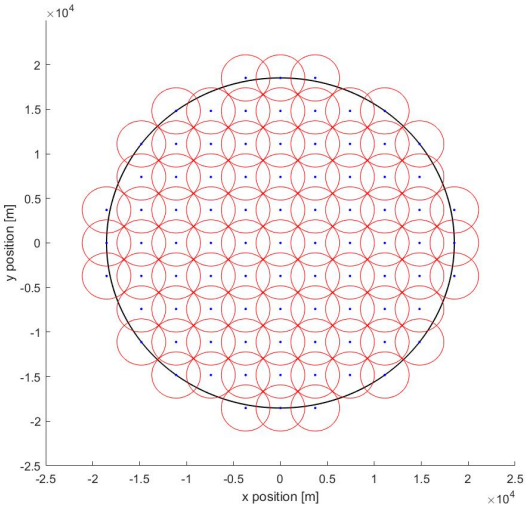

Figure 6: Distribution of 89 birth model components

9 can not be detected by the RADAR with all 3 bands; target 10 does not have an AIS transceiver that means AIS can not receive any information from this target. The target state at time k is modeled using a 4-D vector $x_k = [p_{x,k}, p_{y,k}, \dot{p}_{x,k}, \dot{p}_{y,k}]^T$, comprising of its x-coordinate, y-coordinate, x-velocity and y-velocity. The motion model in the simulated scenario is given as

$$\pi(x_k|x_{k-1}) = \mathcal{N}(x_k; Fx_{k-1}, Q) \tag{15}$$

with transition matrix F and processing noise Q

$$F = \begin{bmatrix} 1 & 0 & T & 0 \\ 0 & 1 & 0 & T \\ 0 & 0 & 1 & 0 \\ 0 & 0 & 0 & 1 \end{bmatrix}, \quad Q = \sigma^2 \times \begin{bmatrix} T^4/4 & 0 & T^3/2 & 0 \\ 0 & T^4/4 & 0 & T^3/2 \\ T^3/2 & 0 & T^2 & 0 \\ 0 & T^3/2 & 0 & T^2 \end{bmatrix} \tag{16}$$

where T is the sample time, set as 10 seconds to reduce the total time steps during the simulation. The covariance matrix in Q is based on the setting of the linear constant motion model [21] with $\sigma^2 = 0.005$.

The target birth model is a Poisson model with a constant-weighted mixture Gaussian intensity $\lambda^B(x) = w^B \sum_{i=1}^{N^B} p^{B,i}(x)$, where the number of the birth components N^B is 89 and the weight w is 0.03, such that the expectation of the number of new births in the FOV is 2.67 (the product of N^B and w). The state of each new-born target $p^{B,i}$ is Gaussian distributed. In order to consider the new-born targets that both enter the FOV from outside or appear inside the FOV, the mean and covariance of all the birth model components are illustrated in Figure 6. Since the AIS information contains the ship's name and IMO number, this information is directly used as an explicit label for every AIS target. For non-AIS targets, implicit labels are generated comprising the birth time and number. Each target in the FOV has a constant survival probability $P^S = 0.9$, so that the death rate is 0.1.

Different sensors have different properties, such as the time-constant probabilities of target detection P^D, standard deviation σ for Gaussian measurement noise, and clutter intensities λ^c. According to the observation of the RADAR system, the data from AIS has highest probability of detection and lowest clutter rate, while F-heli RADARA has lowest probability of detection and highest clutter rate. F-band RADAR, I-band RADAR are somewhere in between of AIS and F-heli RADAR in terms of these two properties. The values of all different properties

	F-band RADAR	I-band RADAR	F-heli RADAR	AIS
P^D	0.9	0.8	0.7	0.99
σ	20	20	20	5
λ^c	2	5	10	1

Table 1: Different Sensor Properties

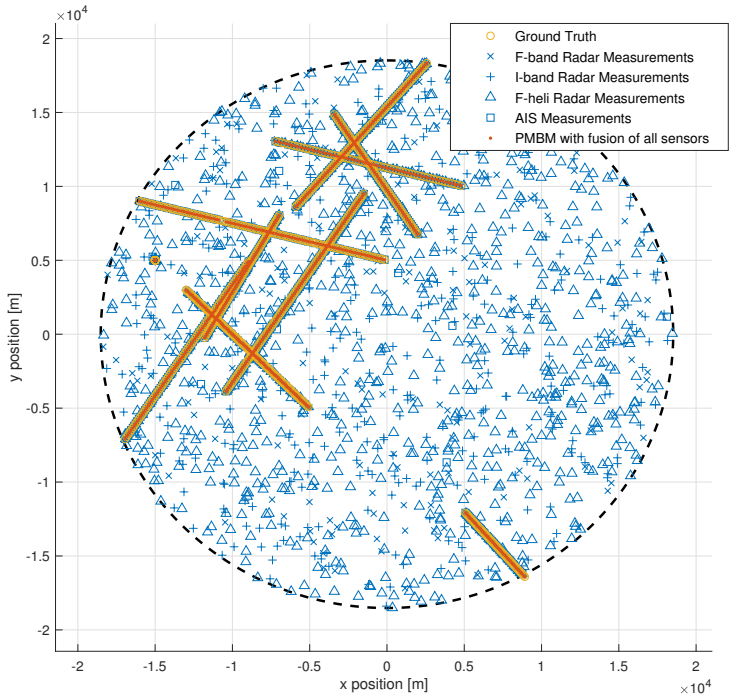

Figure 7: Result of fusion of RADAR and AIS using PMBM filter

are listed in Table 1. The general position measurement model for all sensors at time k is given as

$$z_{s,k} = Hx_k + R \tag{17}$$

with measurement matrix H and measurement noise R

$$H = \begin{bmatrix} 1 & 0 & 0 & 0 \\ 0 & 1 & 0 & 0 \end{bmatrix}, \quad R = \begin{bmatrix} v_{k,1} \\ v_{k,2} \end{bmatrix} \tag{18}$$

In 18, $v_{k,1}$ and $v_{k,2}$ are mutually independent zero-mean Gaussian noise with the standard deviation σ. Three different orders of fusion are studied to show the influence of order to the sequential fusion of multi-sensor fusion PMBM:

- Sequential fusion order 1: AIS → F-band RADAR → I-band RADAR → F-heli RADAR
- Sequential fusion order 2: F-heli RADAR → I-band RADAR → F-band RADAR → AIS
- Sequential fusion order 3: F-band RADAR → I-band RADAR → AIS → F-heli RADAR

The performance for RFS-based filter is especially evaluated by the metric: mean GOSPA[22], which turns out to be a sum of localization error for the properly detected target and cardinality error for missed detection and false alarm, expressed as

$$d_p^{(c,2)}(X,\hat{X}) = \left[min_{\gamma\in\Gamma} \left(\sum_{(i,j)\in\gamma} d(x^i,\hat{x}^j)^p + \frac{c^p}{2}(|X| - |\gamma| + |\hat{X}| - |\gamma|) \right) \right]^{1/p} \tag{19}$$

In 19, the parameters c is set as 100 to fit the scale of distance and p is set as 1 to use the two-dimensional distance. In order to show the number of missed detections and false alarms more intuitively, the results of both missed detections and false alarms are scaled back to the actual number, as shown by the right-side y-axis in Figure 8.

The fusion results of multi-target tracking based on PMBM filter with 100 time steps is given in Figure 7. The performance evaluation using mean GOSPA is given in Figure 8. A comparison of using different fusion orders is shown in Figure 9. The results show:

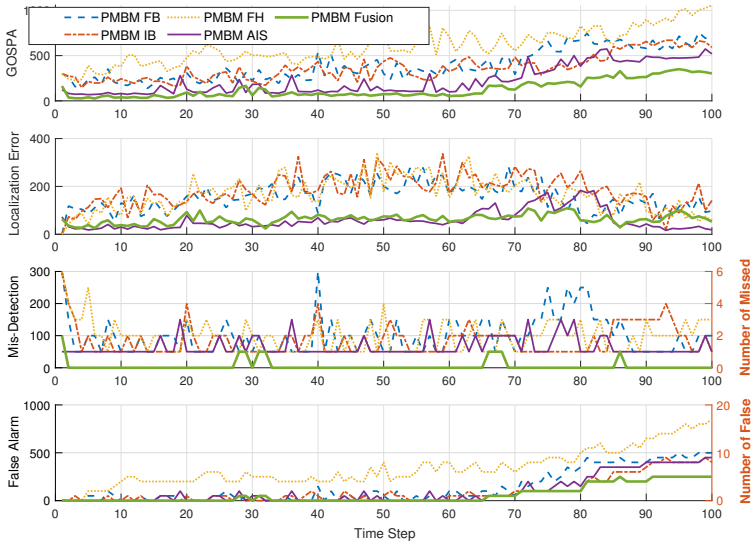

Figure 8: GOSPA results of PMBM filter with single sensor and multi-sensor fusion

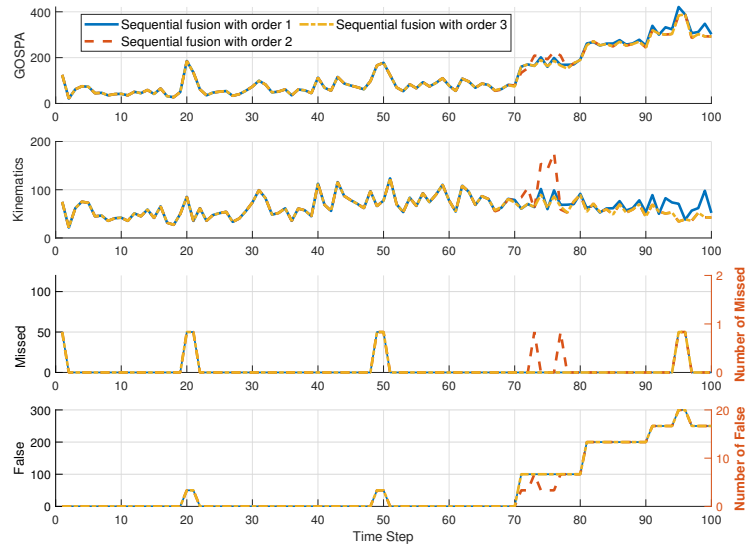

Figure 9: Comparison of sequential fusion with different fusion orders

- The proposed sequential fusion of RADAR and AIS indeed improves the performance of PMBM filter in the studied maritime scenario. It significantly reduces the GOSPA error at least about 40% compared with any single-sensor PMBM. In particular, by applying sequential fusion, the number of missed detections can be reduced to 0 during about 90% simulation time steps, even if part of these targets can not be detected by a certain single sensor. That is, in this scenario, all the targets can be tracked using multi-sensor PMBM with the proposed sequential fusion. The sequential fusion of multi-sensor PMBM filter is able to handle the situations when the information from different sensors conflicts, using a Bayesian way to describe the probability of all situations and extract the most probable one.

- The localization error increases a little during certain time periods by the sequential fusion as compared with only using AIS. That is because AIS data has relatively higher accuracy than RADAR, state uncertainty is simultaneously increased when we try to accept the more possibilities brought by RADAR. Despite this, the localization error using sequential fusion drops significantly from time step 70 to 85 compared to the best result of the single-sensor case(using AIS). It means that a better data association by sensor fusion also helps

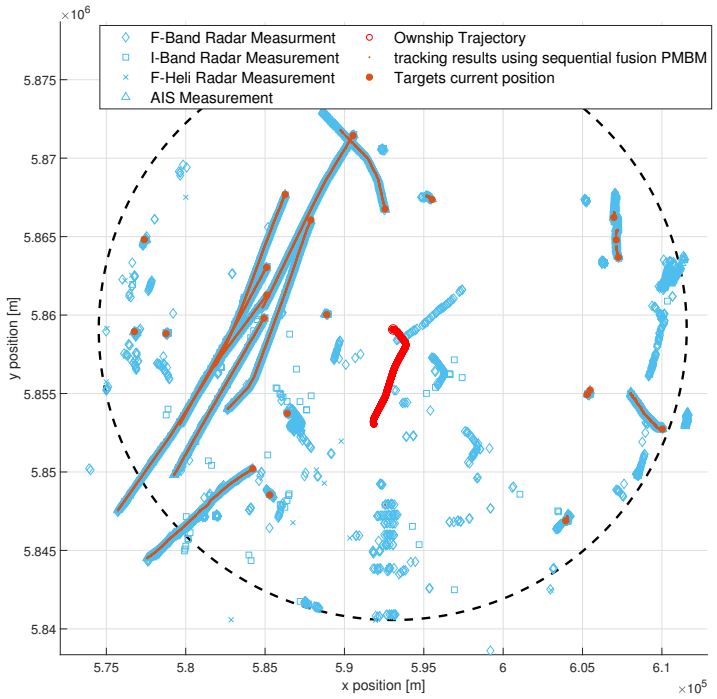

Figure 10: Tracking result using sequential fusion of RADAR and AIS based on PMBM filter in the real multi-target tracking scenario with low RADAR gain

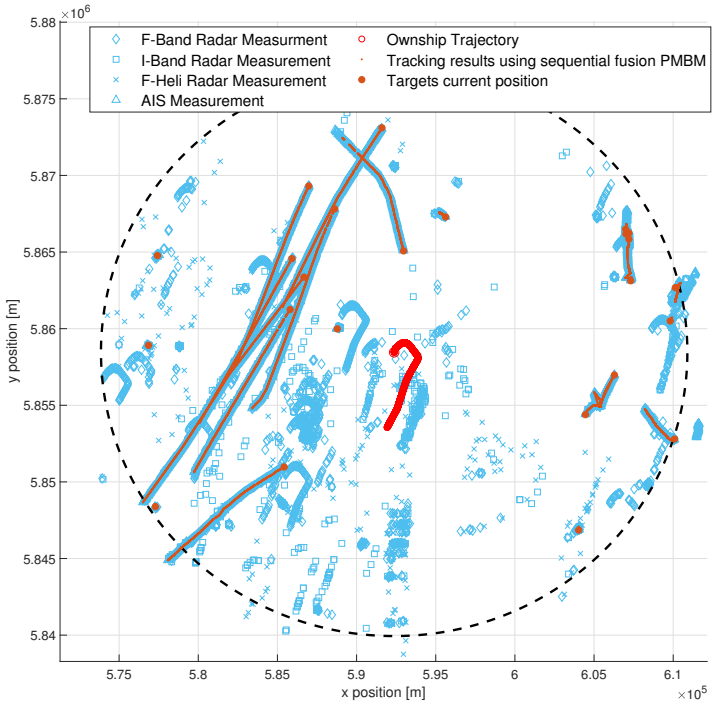

Figure 11: Tracking result using sequential fusion of RADAR and AIS based on PMBM filter in the real multi-target tracking scenario with high RADAR gain

to reduce the localization error when the cardinality is changing.

- Although only the comparison of 3 orders among all the 24 orders is shown in this paper, the result basically meets the theoretical expectations. That is, the fusion order of the sensor does not have much influence on the tracking results. Theoretically, there are no differences with different fusion orders since PMBM has a closed-form solution without any approximations. But due to the post-processing step, such as pruning, recycling, and merging, used to speed up the calculations, it is possible that some correct hypotheses currently having low probabilities are pruned. The small difference occurs when the targets die. On the one hand, starting fusion with F-Heli RADAR (order 2), the one with the highest clutter detection rate and lowest detection probability, two extra missed detections occur after the first death of the targets. On the other hand, the number of false alarms is reduced slightly at a similar time position. Thus, the influence of the fusion order can be omitted with the configuration in this study and the fusion order was used for all other simulations.

- The computational time in the above simulations (AIS, F-Band, I-Band, F-Heli, sequential fusion) using the Monte Carlo method is 18.2 seconds, 35.2 seconds, 149.6 seconds, 468.5 seconds, and 52.3 seconds, respectively, over 100 time steps with the same configuration. For the single-sensor PMBM, the computational time increases rapidly from using AIS to using F-Heli band radar, as the decreasing probability of detection and the increasing clutter rate. Compared to the single AIS and single F-band, the increasing computational time of sequential fusion is not surprising since there are four iterations in each update step. In contrast, compared to the single I-Band and F-Heli, the computational time using sequential fusion is significantly reduced while all the information is used. After splitting to each time step, this computational time of sequential fusion is still acceptable (0.523 seconds per time step) with respect to 1 second sampling time. It is noted that Murty's algorithm was applied for the prediction and update step in this simulation. For the real scenario application with a potentially larger number of targets, a significantly faster implementation is realized by using Gibbs sampling to calculate the joint prediction and update[23].

- In Figure 7, the trajectories of all the targets are calculated and displayed clearly. However, it is observed that there is a gap among the trajectory dots of target 9. Such that the whole trajectory is divided into two tracklets. Even though with the explicit label from AIS, we can still easily associate the two tracklets with the same target, the trajectory gaps of the non-AIS targets might be a problem. In that case, only implicit labels can be used, such that two tracklets can have two different labels. In other words, due to the missed detection, the hypothesis that there are two different targets is more likely than the one-target hypothesis. To avoid this misjudgment, extra post-processing steps can be introduced to merge the tracklets from the obviously same target. Another choice is to estimate the set of trajectories instead of labelling[24], which can be one of the future research direction.

4.3 Application

The proposed multi-sensor PMBM filter with the sequential fusion was applied to a recorded real scenario during a sea trial. Point-target-based dynamic data from the RADAR with all three bands can be captured by an automatic RADAR plotting aid (ARPA). The AIS and RADAR data encoded in the Tracked Target Message (TTM) format were pre-processed into point-target-based dynamic states. Data arriving time of AIS and radars with 3 different bands are different, and AIS and RADAR information are based on different reference systems. Therefore, time and coordinate were synchronized before the fusion. The tracking result based on a 30-minute sailing is illustrated in Figure 10. Compared to the normal human experience-based judgment, targets including static platforms and all the vessels were all picked out and well tracked using sequential fusion. Different clutter rates of 3-band RADAR were tested by changing the degree of enhancement of the RADAR. With a strong enhancement setting, the RADAR detection intensity can be quite strong, as shown in Figure 11. In this case, more ghost targets (clutter) are detected by APRA, which has impacted the tracking performance. As the result shows, some targets are missed, because a high clutter rate leads to lower probabilities of hypotheses that are prone to be pruned during post-processing. Tracklets merging also becomes more challenging due to the high clutter for the non-AIS targets. In addition, it is observed that the distribution of the clutter measurements from the real data is related to our own ship and targets. The reason could be that RADAR echo can be reflected by sea surface and bounces between near targets, and some internal noise of RADAR itself. Thus, the PPP intensity of the clutter model should be determined according to the specific scenarios.

5 Conclusions and further research

In conclusion, this paper applied a sequential approach for RADAR and AIS fusion based on the PMBM filter with the point object assumption. The update of both undetected objects by Poisson Point Process and

detected objects by Multi-Bernoulli Mixture is sequentially iterated with all sensors, while the prediction step is unchanged. Compared to the single-sensor PMBM, the results show that the sequential fusion of RADAR and AIS can significantly improve the tracking performance. In particular, when targets are partly not able to be detected by a certain single sensor, or information from different sensors conflicts, those targets can still be well tracked using sequential fusion. The fusion order does not have much influence on the tracking result, such that the fusion can be achieved even with a random order. That means that, in the case of autonomous sailing, it is not necessary to align the arriving time of RADAR and AIS using this sequential fusion. The computational time is increased (52.3s) but still acceptable compared to the single AIS case (18.2s) with the actual four sensors in this study. However, the computational load will be further increased as the number of sensors increases. Research on the fusion of massive sensors could be one future direction. Tracklets merging is introduced during the post-processing in this study to merge the tracklets from the obviously same target.

This sequential fusion of AIS and RADAR based on PMBM filter was also successfully applied to a real maritime MTT scenario. We also studied the influence of different clutter rates by changing the enhancement degree of RADAR. In different scenarios and environments, clutter rates probably change. Thus, making this multi-sensor PMBM applicable to more scenarios is another potential direction of our future research.

Acknowledgement

The research leading to these results has received funding from the European Union's Horizon 2020 research and innovation programme under the Marie Skłodowska-Curie Grant Agreement No 812.788 (MSCA-ETN SAS). This publication reflects only the authors' view, exempting the European Union from any liability. Project website: http://etn-sas.eu/.

References

[1] Yaakov Bar-Shalom, Fred Daum, and Jim Huang. The probabilistic data association filter. *IEEE Control Systems Magazine*, 29(6):82–100, 2009.

[2] Samuel S Blackman. Multiple hypothesis tracking for multiple target tracking. *IEEE Aerospace and Electronic Systems Magazine*, 19(1):5–18, 2004.

[3] Ba-Tuong Vo and Ba-Ngu Vo. A random finite set conjugate prior and application to multi-target tracking. In *2011 Seventh International Conference on Intelligent Sensors, Sensor Networks and Information Processing*, pages 431–436. IEEE, 2011.

[4] Ronald PS Mahler. *Advances in statistical multisource-multitarget information fusion*. Artech House, 2014.

[5] Ozgur Erdinc, Peter Willett, and Yaakov Bar-Shalom. Probability hypothesis density filter for multitarget multisensor tracking. In *2005 7th International Conference on Information Fusion*, volume 1, pages 8–pp. IEEE, 2005.

[6] Ba-Tuong Vo, Ba-Ngu Vo, and Antonio Cantoni. Analytic implementations of the cardinalized probability hypothesis density filter. *IEEE transactions on signal processing*, 55(7):3553–3567, 2007.

[7] Ba-Tuong Vo, Ba-Ngu Vo, and Antonio Cantoni. The cardinality balanced multi-target multi-bernoulli filter and its implementations. *IEEE Transactions on Signal Processing*, 57(2):409–423, 2008.

[8] Francesco Papi, Ba-Ngu Vo, Ba-Tuong Vo, Claudio Fantacci, and Michael Beard. Generalized labeled multi-bernoulli approximation of multi-object densities. *IEEE Transactions on Signal Processing*, 63(20):5487–5497, 2015.

[9] Jason L Williams. Marginal multi-bernoulli filters: Rfs derivation of mht, jipda, and association-based member. *IEEE Transactions on Aerospace and Electronic Systems*, 51(3):1664–1687, 2015.

[10] Yuxuan Xia, Karl Granstrcom, Lennart Svensson, and Ángel F García-Fernández. Performance evaluation of multi-bernoulli conjugate priors for multi-target filtering. In *2017 20th International Conference on Information Fusion (Fusion)*, pages 1–8. IEEE, 2017.

[11] Tiancheng Li and Kai Da. Best fit of mixture for distributed poisson multi-bernoulli mixture filtering. 2020.

[12] Dan Hermann, Roberto Galeazzi, Jens Christian Andersen, and Mogens Blanke. Smart sensor based obstacle detection for high-speed unmanned surface vehicle. *IFAC-PapersOnLine*, 48(16):190–197, 2015.

[13] Øystein Kaarstad Helgesen, Edmund Fϕrland Brekke, Hkon Hagen Helgesen, and Øystein Engelhardtsen. Sensor combinations in heterogeneous multi-sensor fusion for maritime target tracking. In *2019 22th International Conference on Information Fusion (FUSION)*, pages 1–9. IEEE, 2019.

[14] Cong-Thanh Do, Tran Thien Dat Nguyen, and Weifeng Liu. Tracking multiple marine ships via multiple sensors with unknown backgrounds. *Sensors*, 19(22):5025, 2019.

[15] Martin Michaelis, Philipp Berthold, Daniel Meissner, and Hans-Joachim Wuensche. Heterogeneous multi-sensor fusion for extended objects in automotive scenarios using gaussian processes and a gmphd-filter. In *2017 Sensor Data Fusion: Trends, Solutions, Applications (SDF)*, pages 1–6. IEEE, 2017.

[16] Kai Lin, Yihui Li, Jinchuan Sun, Dongsheng Zhou, and Qiang Zhang. Multi-sensor fusion for body sensor network in medical human–robot interaction scenario. *Information Fusion*, 57:15–26, 2020.

[17] Ronald Mahler. Phd filters of higher order in target number. *IEEE Transactions on Aerospace and Electronic systems*, 43(4):1523–1543, 2007.

[18] Athanasios Papoulis and S Unnikrishna Pillai. *Probability, random variables, and stochastic processes*. Tata McGraw-Hill Education, 2002.

[19] Ángel F García-Fernández, Jason L Williams, Karl Granström, and Lennart Svensson. Poisson multi-bernoulli mixture filter: direct derivation and implementation. *IEEE Transactions on Aerospace and Electronic Systems*, 54(4):1883–1901, 2018.

[20] Sharad Nagappa and Daniel E Clark. On the ordering of the sensors in the iterated-corrector probability hypothesis density (phd) filter. In *Signal Processing, Sensor Fusion, and Target Recognition XX*, volume 8050, page 80500M. International Society for Optics and Photonics, 2011.

[21] Samuel Blackman and Robert Popoli. Design and analysis of modern tracking systems(book). *Norwood, MA: Artech House, 1999.*, 1999.

[22] Ángel F García-Fernández, Yuxuan Xia, Karl Granström, Lennart Svensson, and Jason L Williams. Gaussian implementation of the multi-bernoulli mixture filter. In *2019 22th International Conference on Information Fusion (FUSION)*, pages 1–8. IEEE, 2019.

[23] Ba-Ngu Vo and Ba-Tuong Vo. An implementation of the multi-sensor generalized labeled multi-bernoulli filter via gibbs sampling. In *2017 20th International Conference on Information Fusion (Fusion)*, pages 1–8. IEEE, 2017.

[24] Ángel F García-Fernández, Lennart Svensson, Jason L Williams, Yuxuan Xia, and Karl Granström. Trajectory poisson multi-bernoulli filters. *arXiv preprint arXiv:2003.12767*, 2020.